Ocean mixing, Internal tides and Tidal power

Chris Garrett

19 June 2008

1 Ocean mixing and Internal tides

1.1 Introduction

Mixing of the oceans ultimately occurs through molecular diffusion, though it is driven by fluctuations in the velocity, temperature and salinity on length scales down to 1 mm that cannot be resolved in large 3D numerical models which typically have a resolution of the order of 10 km $\times$ 10 km $\times$ 100 m. It will be many, many, years before resolution can be improved to resolve the small scale turbulence which causes mixing; as a result accurate parameterisations of the small scale processes are necessary.

Sub-grid scale mixing in the ocean may be likened to the influence of clouds or ice crystals in the atmosphere - they are unresolved in any large scale model, and yet have a very important effect on the overall dynamics. The mixing processes in the ocean are less obvious without injecting artificial dyes but likewise play an important role in the global oceanic circulation.

The general framework to parameterise mixing is usually to represent the eddy flux of a scalar C as a tensor multiplying the gradient of the mean $\bar{C}$;

$$\overline{u_i' C'} = -T_{ij} \frac{\partial \bar{C}}{\partial x_j}, \tag{1}$$

where u_i' and C' are the small scale fluctuations of the velocity components and the scalar. The antisymmetric part of T_{ij} has an associated 'skew flux' $\mathbf{D} \times \nabla \bar{C}$ which is parallel to surfaces of constant $\bar{C}$. The symmetric part of T_{ij} may be diagonalised and thus represents diffusion parallel to some principal axes. The skew flux and large isopycnal diffusivities are likely to be a consequence of stirring by mesoscale eddies; the flux of more interest for ocean mixing is that *across* isopycnals, i.e. the diapycnal flux, and this is parameterised in terms of an eddy diffusivity K_v. Some possible causes for concern with this approach were noted; there are an implicit assumptions that there is some local 'mixing length' and that there is a spectral gap between the mean and fluctuations; in reality this distinction may be rather blurred. Nevertheless, quantifying mixing with a diffusivity is the common method used in numerical models; the question is, how should it vary in space and time, and what causes these variations?

Knowledge of diapycnal mixing comes from

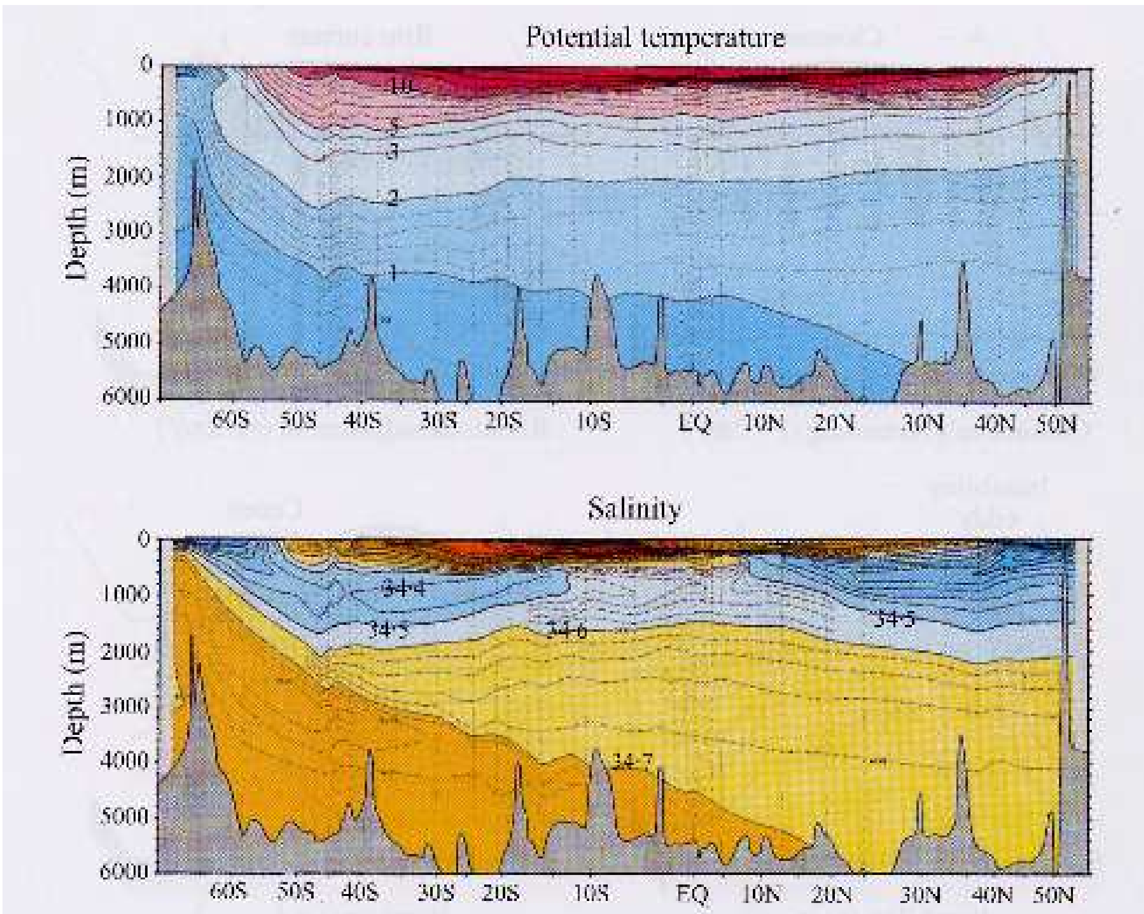

Figure 1: GEOSECS section of the potential temperature and salinity in a meridional cross section of the Pacific. The observed stratification, combined with estimates of the circulation, can be used to infer how much mixing must occur.

- Inference - Balancing budgets for confined regions such as deep basins, using measurements of the inflow together with simple models to infer parameters;
- Measurements - for instance, injecting dye or measuring small scale variations in temperature and velocity;
- Process Studies - modeling and quantifying the physical processes such as internal wave formation and breaking which give rise to the mixing.

If models aim to represent realistic physics and therefore be able to predict future behaviour, it is important that they take account of the processes rather than just using inferred or measured values. Having the right spatially varying *numbers* is important, but for future prediction we need *formulae* too, so that we take account of any feedbacks in the system.

1.2 Inference

Measurements of temperature and salinity through the depth of the ocean suggest that mixing occurs at all depths, not just in the well mixed surface boundary layer. This results in a stratified interior of the ocean where, in the absence of mixing one would expect an almost uniform core with a much shallower boundary region near the surface where all the mixing occurs. The essential dynamics of turbulent mixing in upwelling regions might be expressed loosely as

$$w\frac{\partial \bar{C}}{\partial z} = \frac{\partial}{\partial z}\left(K_v \frac{\partial \bar{C}}{\partial z}\right), \tag{2}$$

from which, if we can estimate the upwelling rate w, and measure the profile $\bar{C}$ (be it temperature, density or salinity), we can infer an average value of the diffusivity K_v. This has been done (Munk 1966, Munk and Wunsch 1998), and suggests a global average value of $K_v \simeq 10^{-4}$ m^2 s^{-1}, at least below the top 1 km or so of the ocean. This figure must be a reflection of the energy input to the oceans.

More local estimates for K_v can also be made by measuring the flux and water properties of flow into deep basins in which water properties are also known. This gives an estimate for the rate of mixing which must occur within the basin and allows an average K_v to be calculated. Typically this also gives values on the order of 10^{-5} to 10^{-4} m^2 s^{-1}. It is not clear from such integrated estimates, however, *where* the mixing occurs - is it in the ocean interior or does it all occur near the boundaries?

1.3 Measurements

Direct observations of mixing come from dye tracer experiments (Ledwell et al. 1998), in which inert dye was released at a specific depth in the ocean and the vertical spread of this dye over time was measured. This suggests that the diffusivity in the open ocean should be on the order of $K_v \sim 10^{-5}$ m^2 s^{-1}, rather less than the inferred global average, though at shallower depths than those to which the global estimates apply, so that there is not a contradiction.

The kinetic energy dissipated can be calculated from measuring the small scale (<cm) variations in the velocities;

$$\epsilon = \nu|\nabla \mathbf{u}|^2. \tag{3}$$

In the stratified ocean, a fraction of this dissipation, often called the mixing efficiency Γ, is used to increase the potential energy of the fluid by raising the centre of mass of the fluid. Γ is generally taken to be around 0.2. The energy transferred to potential energy is also related to the diffusivity by

$$\Gamma\epsilon = K_v N^2, \quad N^2 = -\frac{g}{\rho}\frac{\partial\rho}{\partial z}, \tag{4}$$

so that if detailed measurements of the velocity on the small scale can be made, a value for the diffusivity K_v can be inferred. However it is unclear if Γ should be a universal constant or should depend upon conditions; in particular it may depend on the stratification N compared with the typical frequency of the waves and also, perhaps, on a parameter describing the strength of wave breaking.

The diffusivities inferred from measuring ϵ are around 10^{-5} m^2 s^{-1} in the open ocean, but show large spatial variations and are more like 10^{-4} m^2 s^{-1} in the deep ocean over regions of rough bottom topography. This suggests that the inferred globally averaged abyssal diapycnal mixing of several 10^{-4} m^2 s^{-1} may be concentrated in localised regions near boundaries or above rough topographies.

1.4 Biological considerations

There was a suggestion from Bill Dewar (Dewar et al. 2006) that a significant proportion of the mixing in the ocean might be caused by the movement of marine animals, particularly zooplankton, which are known to travel up and down depths of more than 1 km every day to feed and escape predators. Large numbers of zooplankton, which tend to move in clouds several hundreds of metres wide, could generate turbulence on a large scale and cause mixing well below the surface mixed layer. It is estimated that around 63 TW is generated by marine animals, and that around 1% of this could be transferred to mechanical energy. Given that overall the mixing of the oceans is thought to require around $2 - 3$ TW, this may not be an insignificant contribution, though it has so far been viewed with a degree of scepticism.

1.5 Internal waves

The greater mixing occurring over rough regions of the bed may indicate that it is the result of internal wave interactions; the waves are generated by flow over the bed and propagate up into the ocean core, where non-linear interactions result in overturning and turbulent mixing.

A method developed by Henyey el al. (1986) attempts to use internal wave theory to infer dissipation rates from measurements of shear and strain over length scales of 10 m. This requires some assumptions on scale separation, but seems to produce the expected results reasonably well in the open ocean. It allows ϵ and hence K_v to be estimated over much larger regions, since the velocity need only be measured at 10 m rather than cm intervals. The results are typically consistent with $K_v \approx 10^{-5}$ m^2 s^{-1}.

The general impression built up from these various inferences and measurements is that energy for mixing is radiated to the ocean interior through internal waves generated both at the surface (by the wind) and at the bottom (by tidal currents over rough topography;

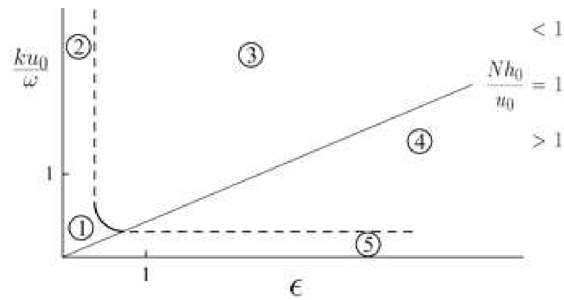

Figure 2: Parameter space for deep-ocean internal tide generation. ϵ is the ratio of bottom slopes to the internal ray slope, and ku_0/ω is the ratio of the tidal excursion to the roughness scale. See Garrett and Kunze, 2007.

internal tides have been visualised as surface waves near Hawaii using satellite measurements (Egbert and Ray, 2000)). Wave-wave interactions set up horizontal currents which lead to overturning and eventually turbulent mixing. Questions arise as to how much of this energy comes from the different sources, and how to parameterise its transfer to the mixing regions.

The energy flux from the wind into near-inertial waves which can propagate below the surface mixed layer varies seasonally and is very dependent on latitude - most of the energy input from this source is at mid latitudes, particularly over the Southern Ocean (Alford 2001, Park et al. 2005). The input is estimated through a combination of satellite and drifter data and numerical models, and it is found that on the order of 1 TW is transmitted from the wind to near-inertial motion.

The energy derived from the barotropic tides has been estimated using satellite data by Egbert and Ray (2001). The tidal elevations can be measured and, through comparison with model simulations, the amount of damping at the ocean floor can be inferred; this is found to occur not just in shallow water off the coasts but also in the open ocean, particularly in regions of rough bottom topography. The estimated power that can be transferred to internal wave generation by this method is around 1 TW globally. It should be noted that Egbert and Ray's method is not accurate in shallow water and may give misleading results in shallow coastal areas.

1.6 Generating internal waves from the tide

The generation of internal tides (that is, internal waves of tidal frequency ω) from barotropic flow over rough topography $h(\mathbf{x})$ depends on several key parameters (Garrett and Kunze, 2007); the ratio ku_0/ω of the length of tidal excursions to horizontal roughness scale, the ratio ϵ of bottom slopes to the internal ray slope, and the ratio of topographic height to the ocean depth. For a deep ocean, there are several different regimes (figure 2) depending on whether none, both or one of ϵ and ku_0/ω are small. The easiest to analyse is when ϵ is small, allowing a linear theory (Bell, 1975). When ku_0/ω is small there are singularities at critical bed slopes, where $\epsilon = 1$ (Balmforth et al. 2002).

Many areas of the ocean such as the Mid-Atlantic Ridge have subcritical slopes and ϵ is small, so the linear theory can be applied. Most of the energy flux into internal tides is in low modes (St. Laurent and Garrett, 2002). With the linear theory, the vertical energy flux from the bottom can be relatively easily calculated, and for a sinusoidal bed $h = h_0 \sin kx$ is

$$F = \frac{1}{4}\frac{\rho}{\omega}\left[(N^2 - \omega^2)(\omega^2 - f^2)\right]^{1/2} k u_0^2 h_0^2. \tag{5}$$

An interesting question one could pose is, supposing this energy flux is dissipated (by internal wave breaking, causing mixing) over some vertical length scale (which could itself depend on the energy flux and N), what happens as the stratification (measured by N^2) changes? Since the energy dissipation causes mixing which alters the stratification, it is of interest whether increasing N^2 causes more mixing which reduces the stratification and would therefore be stable, or whether it causes less mixing, which increases the stratification and causes an unstable positive feedback.

1.7 Transfer of energy and internal wave breaking

The bulk of the energy of internal waves at the M_2 tidal frequency (semi-diurnal) is in low modes which can propagate over long distances from their generation site before breaking up by interactions with each other or with fixed boundaries. It is estimated that up to 1 TW of the 3.5 TW tidal power dissipated by the ocean could be 'available' by this method to cause mixing in the ocean interior. The fact that the energy can be generated in one place and transported to another place before dissipating makes it difficult to parameterise. It will be important to understand where and how this mixing occurs; whether the energy flux in low modes breaks down into shorter waves through wave-wave interactions or by bouncing off rough topography, or whether it is transported to continental slopes where it is possible that the energy could be 'wasted' in mixing the water in a bottom boundary layer which is already well mixed.

The take home message is that mixing parameterisations (for large scale numerical models this essentially means eddy diffusivities) cannot be based only on purely local conditions. There is much spatial variability which can be measured and included, but understanding and parameterising the *processes* which give rise to this is important if models hope to be truly predictive.

2 Energy from the sea?

2.1 Introduction

The oceans play a major role in global energy issues, both in terms of their current uses and role in the carbon cycle, and in their potential to be exploited as an alternative energy source in the future. Currently large amounts of oil and gas are recovered offshore, ocean water is used for cooling nuclear power plants (and the oceans were once used for nuclear waste disposal), and there is an increasing number of offshore wind farms being developed.

Wave power has been suggested as a means of extracting energy from the surface of the ocean but, apart from small local projects, will probably not be able to produce energy on a significant scale. Tidal power has somewhat more potential for larger scale projects and probably offers more opportunities as a significant 'new' power source. Assessing how much energy can be extracted from such projects and where they should be placed is therefore of great interest. There may also be the possibility to use larger scale circulatory currents, such as the Gulf Stream, to supply useful amounts of power, and the feasibility of such schemes poses a large range of fluid dynamical questions.

2.2 A global perspective

The tides caused by the motion of the moon and sun are estimated to supply 3.7 TW (3.7×10^{12} W) of power which must be dissipated by transfer to kinetic, potential and internal energy of the earth, atmosphere and oceans (Munk and Wunsch, 1998). The vast majority of this energy transfer, approximately 3.5 TW, occurs in the oceans, initially as surface tides, with energy eventually being dissipated through bottom friction and internal wave formation leading to localised turbulence and mixing. As a comparison, human power usage is around 15 TW, a large power station generates around 1 GW, the total wind dissipation in the atmosphere is around 1000 TW, and insolation provides nearly 10^5 TW (advances in solar power are presumably therefore the most promising way forward).

An important first question when we consider large scale tidal power generation is how much of this we can feasibly tap into without altering the tidal dynamics so much that we start to reduce the available power. A simple model to assess this question was suggested; that is to treat the Earth's oceans as a simple harmonic oscillator with a natural resonant frequency ω_0 which is near to the frequency of tidal forcing ω:

$$\ddot{x} + (\lambda_0 + \lambda_1)\omega_0\dot{x} + \omega_0^2 x = F(t) \equiv \cos\omega t. \tag{6}$$

The natural dissipation of the oceans is written as the damping force $\lambda_0\omega_0\dot{x}$, and the term $\lambda_1\omega_0\dot{x}$ is the extra dissipation which we might impose through tidal power generation. $F(t)$ is the tidal forcing at frequency ω. The average power dissipated from the system is

$$P_{total} = \overline{(\lambda_0 + \lambda_1)\omega_0\dot{x}^2} = \overline{F\dot{x}}, \tag{7}$$

where the overbars denote the average over a cycle. The power generated for human use is a fraction of this;

$$P_1 = \frac{\lambda_1}{\lambda_0 + \lambda_1} P_{total}, \tag{8}$$

and the question is how does this vary as we vary λ_1?

The solution of (6) is

$$x(t) = \frac{(\omega_0^2 - \omega^2)\cos\omega t + (\lambda_0 + \lambda_1)\omega\omega_0 \sin\omega t}{(\omega_0^2 - \omega^2)^2 + (\lambda_0 + \lambda_1)^2\omega^2\omega_0^2}, \tag{9}$$

giving

$$P_{total} = \frac{1}{2}\frac{(\lambda_0 + \lambda_1)\omega_0\omega^2}{(\omega_0^2 - \omega^2)^2 + (\lambda_0 + \lambda_1)^2\omega^2\omega_0^2}, \tag{10}$$

and

$$P_1 = \frac{1}{2}\frac{\lambda_1\omega_0\omega^2}{(\omega_0^2 - \omega^2)^2 + (\lambda_0 + \lambda_1)^2\omega^2\omega_0^2}. \tag{11}$$

As more artificial dissipation (λ_1) is added at first it produces more power, but eventually the system saturates and then as more friction is added the power output decreases. P_1 has

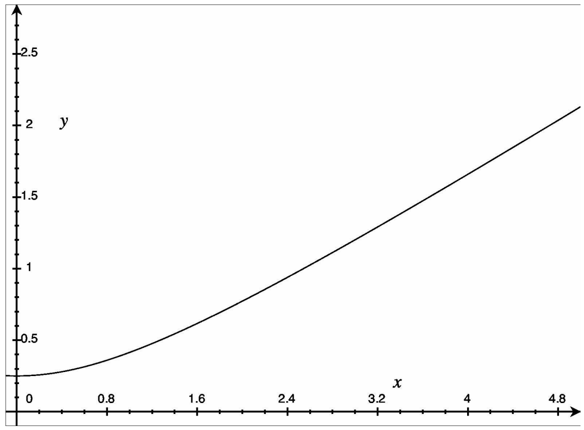

Figure 3: Fraction of current tidal dissipation which could be used for human energy sources as a function of the distance from resonance x of the tides, from (14). Dominant tidal modes are likely to be close to resonance, so the relevant section of this graph is where x is small and the ratio is close to 1/4.

a maximum when $(\omega_0^2 - \omega^2)^2 + (\lambda_0 + \lambda_1)^2\omega^2\omega_0^2 = 2(\lambda_0 + \lambda_1)\lambda_1\omega_0^2\omega^2$, and the power then generated is

$$P_{max} = \frac{1}{4\lambda_0\omega_0}\frac{1}{1 + (1 + x^2)^{1/2}}, \tag{12}$$

where

$$x = \frac{\omega_0^2 - \omega^2}{\lambda_0\omega_0\omega}, \tag{13}$$

is a parameter which describes how far the tidal forcing is from the resonant frequency. Ocean tides are thought to be close to resonance, so that x is a small parameter. This compares with the natural tidal dissipation P_{nat} (that is, (10) with $\lambda_1 = 0$) by a factor

$$\frac{P_{max}}{P_{nat}} = \frac{1 + x^2}{2[1 + (1 + x^2)^{1/2}]}, \tag{14}$$

which is symmetric in x so that we have only considered positive values in figure 3.

Near resonance, x is small and the largest amount we can hope to extract is around 1/4 of the naturally dissipated energy (3.5 TW). The tides therefore offer a considerable potential source of energy if we can find the engineering capabilities and suitable locations to extract this energy.

2.3 Tidal power engineering

Conventional tidal power projects make use of an existing bay by building a barrage across the bay entrance which traps the water in the bay at high tide. Once the level of the water outside the bay has fallen the water is released through turbines, the energy coming from the drop in potential energy of the water. The bay is thus filled and emptied during every tidal cycle. If the tidal range is a depth $2a$ and the bay has a surface area A_s, then the maximum potential energy release as the water passes through the turbines is

$$\frac{1}{2}\rho_w g A_s (2a)^2, \tag{15}$$

and since this can only occur once per tidal cycle (maybe twice if the process is repeated on the flood tide, but we ignore this possibility) the average power produced is

$$\frac{\omega}{\pi}\rho_w g A_s a^2, \tag{16}$$

where $\omega \approx 2\pi/12.4\ \mathrm{h}^{-1}$ is the frequency of the dominant M_2 tide. For a reasonably large basin of area $A_s = 100\ \mathrm{km}^2$ and a tidal range of $2a = 4$ m this gives about 240 MW. The La Rance facility in France is an example of this type of project in operation and several other possible sites have been mooted. Naturally the obvious place to build such projects is in areas where the tidal range is very large such as the Bay of Fundy in Eastern Canada and the Severn estuary in the UK. Unfortunately this property means that these locations are also considered important ecological sites and there is much debate as to whether the benefits of developing large schemes can justify the loss of unique habitats and ecosystems.

Another possibility, alongside or instead of using bays and estuaries, is to place turbines in channels where there are strong tidal currents and to use the existing currents to drive the turbines. Many such places have been suggested and the 'rights' to develop tidal schemes in some such locations are being claimed (in Puget Sound for instance). Of course, these schemes also have potential ecological problems as well as posing problems for shipping and fishing.

2.4 Extracting power from a tidal channel

As our ability to build and position large submarine turbines increases it is important to be able to assess where the best place to position the turbines is, and how many should be used in order to make the most efficient use of the available energy. Just as on the global scale, if too many turbines are used in one location the tidal currents will be reduced and the power output will decrease. Maximising the power output from a channel means optimising the number and position of turbines. If channels converge or diverge it is important to consider what effect building a turbine in one location will have on the flow in other channels, and similarly if currents are going to be utilised in conjunction with damming bays or estuaries then the interaction between the different schemes needs to be carefully considered.

The power available from any given channel is often misleadingly estimated by measuring the kinetic energy flux through a cross-section. If flow at velocity u occurs along a channel of area A between two large basins then the kinetic energy flux through the cross-section is

$$\frac{1}{2}\rho_w A u^3. \tag{17}$$

This will be a misleading value to quote as the power which could be extracted from a particular location since it is highly dependent on where in the channel it is measured and there is no reason to assume that, if a turbine is placed at the location with the greatest flux, the same power will be generated by the turbine. Moreover, if more than one turbine is placed in the same channel one clearly cannot hope to extract the same energy flux twice or more! Interpreting maps of potential turbine sites must therefore be done with due caution.

The problem of maximising the power output from flow down a channel can be considered most simply by looking at the effect of a 'fence' of turbines constructed across the channel (whether this would be feasible for shipping etc. is questionable, but calculations suggest that a complete fence may be the most efficient option for power generation).

For flow along a channel of cross section $A(x)$ at velocity $u(x,t)$, a one dimensional force balance for the flow is

$$\frac{\partial u}{\partial t} + u\frac{\partial u}{\partial x} + g\frac{\partial \zeta}{\partial x} = -F, \tag{18}$$

in which ζ is the surface elevation and F is the friction which may be written in terms of a drag coefficient C_D as

$$F = \frac{C_D u^2}{h} + F_{turb}. \tag{19}$$

F_{turb} is the additional friction introduced by the turbine, and the quantity of interest is the power dissipated by the turbine,

$$P = \rho_w \overline{Q F_{turb}}, \tag{20}$$

where the overbar denotes a space-time average. Q here is the volume flux Au, and if we assume that the channel is short compared to the wavelength of the tide (likely to be hundreds of kilometres) then volume conservation requires that this volume flux is independent of distance along the channel.

We imagine the flow in the channel is driven by the changing elevation of the basins at either end and we write $\Delta\zeta(t)$ as this head difference (note that this could vary between positive and negative over the tidal cycle). We can think of prescribing this head difference, e.g. $\Delta\zeta = a\cos\omega t$, as the tidal forcing in this model. With $u(x,t) = Q(t)/A(x)$, we integrate (18) over the length of the channel L to get

$$c\frac{dQ}{dt} = g\Delta\zeta - \alpha Q|Q| - F_{turb}, \tag{21}$$

where

$$c = \int_0^L \frac{1}{A}\,\mathrm{d}x, \quad \alpha = \frac{1}{2}\frac{1}{A_L^2} + \int_0^L \frac{C_D}{hA^2}\,\mathrm{d}x, \tag{22}$$

A_L is the cross-sectional area at the outlet, where the flow separates, and we assume that the flow at the inlet is simple sink flow so that there is no additional term from there.

The question of interest is what happens to the generated power P as we vary the friction provided by the fence of turbines F_{turb}. In general this requires knowing how this turbine drag depends on the flow rate (e.g. a linear or quadratic dependence), and (21) must then be solved to find the maximum power according to (20). A simple quasi-steady limit can be considered; if the acceleration is unimportant then the turbine-free channel has

$$Q(t) = \left(\frac{g\Delta\zeta(t)}{\alpha}\right)^{1/2}. \tag{23}$$

When a turbine is introduced, Q will differ from this, but how it differs will depend on the form of F_{turb}. In the quasi-steady state the power can be written

$$P = \overline{\rho_w Q(g\Delta\zeta - \alpha Q|Q|)}, \tag{24}$$

and we can therefore find the maximum possible power available by finding the Q which makes this largest. This happens when

$$Q(t) = \left(\frac{g\Delta\zeta(t)}{3\alpha}\right)^{1/2}, \tag{25}$$

and the power is then

$$P = \overline{\frac{2}{3^{1/2}}\rho_w g\Delta\zeta(t)\left(\frac{g\Delta\zeta(t)}{\alpha}\right)^{1/2}} \approx 0.21\rho_w gaQ_{max}, \tag{26}$$

if $\Delta\zeta = a\cos\omega t$ and $Q = Q_{max} = (ga/\alpha)^{1/2}$. In this case Q is reduced to $1/3^{1/2} \approx 0.58$ of its natural value and 2/3 of the head drop $\Delta\zeta$ is associated with the operation of the turbines.

Including acceleration and using different forms for the turbine drag gives the general result that

$$P = \gamma\rho_w gaQ_{max} \tag{27}$$

with the numerical factor γ somewhere between 0.19 and 0.24 (Garrett and Cummins, 2005).

This analysis suggests that if a fence of turbines is built, the location along the channel is unimportant, provided there is only one such fence. This is in contrast to the simplistic power estimate (17); we can compare the above result with that estimate in the case when the drag coefficient C_D is small so that from (26),

$$P = \frac{2}{3^{1/2}}\rho_w\alpha\overline{\left(\frac{g\Delta\zeta(t)}{\alpha}\right)^{3/2}} \approx \frac{2}{3^{1/2}}\ \frac{1}{2}\rho_w A_L\overline{u_L{}^3}, \tag{28}$$

where u_L is the exit velocity in the natural state (23). The predicted maximum power is a fraction $2/3^{1/2} \approx 0.38$ of that predicted naively from the kinetic energy flux at the channel outlet. In general, it is likely that (17) will give an overestimate of the available power.

Detailed numerical calculations have been made to check some of these assumptions and to assess the potential in more complex situations such as the Johnstone Strait in British Columbia. Here the flow splits between different tidal passages and introducing a turbine in one will cause more of the flow to be diverted into other passages, thus reducing the maximum power available to the turbine. This emphasises the importance of assessing the impact of tidal schemes over large areas to avoid overstating the potential of these schemes.

2.5 Extracting power from a tidal bay

A very similar analysis can be carried out for flow into and out of a bay, when turbines can be located across the mouth of the bay and increase the friction there. In this case the volume of water in the bay must be conserved so that the height of the water in the bay $\zeta(t)$ will evolve separately, with a phase lag, from the forcing height $\zeta_0(t)$ outside the bay. A corresponding model might be

$$c\frac{dQ}{dt} = g(\zeta_0 - \zeta) - \alpha Q|Q| - F_{turb}, \quad A_s\frac{d\zeta}{dt} = Q, \tag{29}$$

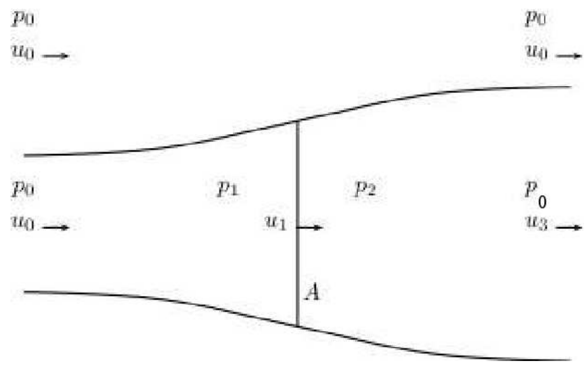

Figure 4: Steamtube passing through a turbine of cross-section A, across which the flow is u_1 and there is a pressure drop $p_1 - p_2$, so that the drag on the turbine is $F = (p_1 - p_2)A$. The background flow is u_0.

in which we attempt to maximise the power

$$P = \overline{\rho_w Q F_{turb}}, \tag{30}$$

by choosing the optimum amount of turbine friction.

With some assumptions about the form of the turbine drag, the maximum power is again found to be

$$P = \gamma \rho_w g a Q_{max}, \tag{31}$$

where $\gamma \approx 0.24$ is a factor which might vary between 0.19 and 0.26, a is the tidal amplitude, and Q_{max} is the maximum flow in the undisturbed state. This gives a power 0.76 times the reference value (16) for a conventional basin scheme in a basin with no natural friction in the entrance. This maximum however occurs when the reduction of the tidal range in the bay is 74% (there is also a change in the phase shift between bay and outside). A scheme such as this therefore has substantial benefits for ecosystems since the natural semidiurnal filling and emptying of the bay is maintained with relatively little alteration.

For both tidal channels and bays, we can conclude from these simple analyses that the maximum power obtainable with a fence of turbines is given approximately by (31) with $\gamma = 0.22$ in terms of the natural tidal amplitude a and maximum flow rate Q_{max}.

2.6 Fences vs. individual turbines

Complete barrages of turbines are probably unfeasible for a number of reasons, so it is of interest what power is lost by using isolated turbines or an array of turbines, when energy is dissipated in the mixing of the wake from each turbine.

The power on an isolated turbine in an infinitely wide channel can be estimated by expressing the force on the turbine in two ways - one using the change in momentum flux across the turbine, the other using Bernoulli's equation for the streamtube which passes through the turbine, as shown in figure 4. This gives

$$p_0 + \frac{1}{2}\rho_w u_0^2 = p_1 + \frac{1}{2}\rho_w u_1^2, \quad p_2 + \frac{1}{2}\rho_w u_1^2 = p_0 + \frac{1}{2}\rho_w u_3^2, \tag{32}$$

whence

$$p_1 - p_2 = \frac{1}{2}\rho_w(u_0^2 - u_3^2), \tag{33}$$

and the force on the turbine of area A is

$$F = \frac{1}{2}\rho_w A(u_0^2 - u_3^2), \tag{34}$$

whilst the change in momentum flux gives

$$F = Au_1(u_0 - u_3). \tag{35}$$

Hence $u_1 = (u_0 + u_3)/2$ and the power generated by the turbine can be written as a multiple of the kinetic energy flux through the undisturbed turbine cross-section:

$$P = Fu_1 = \frac{1}{2}(1+r)(1-r^2) \times \frac{1}{2}\rho_w A u_0^3, \quad r = \frac{u_3}{u_0}. \tag{36}$$

This has a maximum when $r = 1/3$, so $u_1 = 2/3\ u_0$, and the power is then 16/27 of the undisturbed kinetic energy flux, the 'Lanchester-Betz' limit. A fence of turbines giving the same head loss would generate power Fu_0, so the proportion of power missed by the isolated turbine as compared to a fence is $1 - u_1/u_0 = 1/3$. This missing power is lost to dissipation as the slow-moving fluid in the turbine wake merges with the faster free stream.

A similar analysis can be applied to an isolated turbine in a finite width channel and the energy loss compared to a fence increases towards a limit of 2/3.

2.7 Other forms of oceanic hydroelectricity

An interesting, although unlikely, suggestion was made concerning the damming of the Red Sea, allowing some of the trapped water to evaporate and then using inflow across the resulting head drop at a rate that balances the evaporation rate of about 1.7 m/yr. The insolation over the Red Sea is around 10^5 GW, so this power would seem to be very well worth harnessing. After 10 years of evaporation however, a head of $H = 17$ m could be exploited to produce power $\rho_w gHQ \approx 4.1$ GW. This is much less than the power causing evaporation, a result of the large latent heat of evaporation - it takes as much energy to evaporate water as to raise it 250 km vertically, so that dropping it a mere 17 m does not seem to be a very effective way of harnessing the power!

In conclusion, tidal power may be a useful, though not hugely abundant, energy source. There are many issues to consider; engineering feasibility, ecological changes, shipping, and careful positioning of schemes are vitally important. The possibility of using tidal currents around headlands or using giant turbines to extract the energy tied up in the global oceanic circulation have been suggested, though not explored fully. It is not clear what impact turbines will have on such 'unenclosed' currents and how effective they would be at harnessing the available power. It is also not clear what impact the increased friction would have upon such currents. It may be the case that less environmental impact is caused by making use of tidal currents in other ways, for instance as an efficient means of cooling nuclear power stations.

References

[1] Alford, M H 2001 Internal swell generation: The spatial distribution of energy flux from the wind to mixed layer near-inertial motions. *J. Phys. Oceanogr.* **31**:2359–2368

[2] Balmforth, N J, Ierley, G R and Young, W R 2002 Tidal conversion by subcritical topography. *J. Phys. Oceanogr.* **32**:2900-2914

[3] Bell, T H 1975 Topographically generated internal waves in the open ocean. *J. Geophys. Res.* **80**:320–327

[4] Bell, T H 1975 Lee waves in stratified flows with simple harmonic time dependence. *J. Fluid Mech.* **67**:705–722

[5] Dewar, W K, Bingham R J, Iverson R L, Nowacek D P, St. Laurent L C and Wiebe P H 2006 Does the marine biosphere mix the ocean? *J. Mar. Res.* **64**:541–561

[6] Egbert, G D and Ray, R D 2000 Significant dissipation of tidal energy in the deep ocean inferred from satellite altimeter data. *Nature* **405**:775–778

[7] Egbert, G D and Ray, R D 2001 Estimates of M_2 tidal dissipation from TOPEX/Poseidon altimeter data. *J. Geophys. Res.* **106**:22475–22502

[8] Garrett, C and Cummins, P 2005 The power potential of tidal currents in channels. *Proc. R. Soc. A* **461** 2563–2572 doi:10.1098/rspa.2005.1494

[9] Garrett, C and Kunze, E 2007 Internal Tide Generation in the Deep Ocean. *Annu. Rev. Fluid Mech.* **39**:57–87

[10] Henyey, F S, Wright, J and Flatté, S M 1986 Energy and action flow through the internal wave field - an eikonal approach. *J. Geopys. Res.* 91:8487–8495

[11] Ledwell, J R, Watson, A J and Law, C S 1998 Mixing of a tracer in the pycnocline. *J. Geophys. Res.* **103**:21499–21529

[12] Munk, W.H. 1966 Abyssal recipes *Deep-Sea Res.* **13**: 707–730

[13] Munk, W and Wunsch, C. 1998 Abyssal recipes II: energetics of tidal and wind mixing. *Deep-Sea Res.* **45** 1976–2009

[14] Park, J J, Kim, K and King, B A 2005 Global statistics of inertial motions. *Geophys. Res. Lett.* **32**: L14612, doi:10.1029/2005GL023258

[15] st St. Laurent, L and Garrett, C 2002 The role of internal tides in mixing the deep ocean. *J. Phys. Oceanogr.* **32**:2882–2899